Journal of NeuroVirology, 8: 225–239, 2002
 ISSN 1355–0284/02 $12.00+.00
DOI: 10.1080/13550280290049679

Choroid plexus macrophages proliferate and release toxic factors in response to feline immunodeficiency virus

DC Bragg,[1] LC Hudson,[2] YH Liang,[3] MB Tompkins,[3] A Fernandes,[1] and RB Meeker[1,2]

[1]*Neurobiology Curriculum and Department of Neurology, University of North Carolina, Chapel Hill, North Carolina;* [2]*Department of Anatomy, Physiological Sciences and Radiology; and* [3]*Department of Microbiology, Parasitology and Pathology, College of Veterinary Medicine, North Carolina State University, Raleigh, North Carolina*

Recent observations have suggested that lentiviruses stimulate the proliferation and activation of microglia. A similar effect within the dense macrophage population of the choroid plexus could have significant implications for trafficking of virus and inflammatory cells into the brain. To explore this possibility, we cultured fetal feline macrophages and examined their response to feline immunodeficiency virus (FIV) or the T-cell-derived protein, recombinant human CD40-ligand trimer (rhuCD40-L). The rhCD40-L was the most potent stimulus for macrophage proliferation, often inducing a dramatic increase in macrophage density. Exposure to FIV resulted in a small increase in the number of macrophages and macrophage nuclei labeled with bromodeoxyuridine. The increase in macrophage density after FIV infection also correlated with an increase in neurotoxic activity of the macrophage-conditioned medium. Starting at 16–18 weeks postinfection, well after the peak of viremia, a similar toxic activity was detected in cerebrospinal fluid (CSF) from FIV-infected cats. Toxicity in the CSF increased over time and was paralleled by strong CD18 staining of macrophages/microglia in the choroid plexus and adjacent parenchyma. These results suggest that lentiviral infection of the choroid plexus can induce a toxic inflammatory response that is fueled by local macrophage proliferation. Together with the observation of increasing toxic activity in the CSF and increased CD18 staining *in vivo*, these observations suggest that choroid plexus macrophages may contribute to an inflammatory cascade in the brain that progresses independently of systemic and CSF viral load. *Journal of NeuroVirology* (2002) **8,** 225–239.

Keywords: human immunodeficiency virus; brain; AIDS; neural culture; neurotoxicity

Introduction

Microglia and macrophages have been consistently implicated as critical components of the neuropathogenesis associated with AIDS. Previous studies have provided extensive documentation that these cells represent the primary targets of lentiviruses within the CNS (Gabuzda *et al*, 1986; Koenig *et al*, 1986; Dow *et al*, 1992; Achim *et al*, 1994; Glass *et al*, 1995; Lane *et al*, 1996; Takahashi *et al*, 1996). Yet, in addition to harboring virus, microglia and macrophages

Address correspondence to Rick Meeker, Department of Neurology, CB# 7025, 6109F Neuroscience Research Bldg., University of North Carolina, Chapel Hill, NC 27599, USA. E-mail: meekerr@glial.med.unc.edu

This work was supported by National Institutes of Health Grant NS33408 and the UNC Center for AIDS Research 9P30 AI50410. The authors would like to acknowledge the excellent technical assistance of Alda Fernandes and Jeremy Boles.

DC Bragg is currently with the Molecular Neurogenetics Unit, Massachusetts General Hospital, Charlestown, Massachusetts.

Received 7 May 2001; revised 12 December 2001; accepted 4 February 2002.

may serve as sources for a number of putative neurotoxins that may contribute to the development of AIDS-related neurodegeneration (Giulian *et al*, 1990; Pulliam *et al*, 1991; Giulian *et al*, 1996; Xiong *et al*, 2000). Numerous studies have reported that lentiviral infection within the CNS is frequently associated with a widespread loss of cortical and subcortical neurons that cannot be explained by direct, neuronal infection (Everall *et al*, 1993; Wiley *et al*, 1991; Meeker *et al*, 1997). Thus, prevailing models of AIDS-related CNS disease have instead proposed that this neuronal cell death may result, at least in part, from chronic exposure to a wide range of soluble factors released from microglia and macrophages following activation by lentiviruses. Support for this hypothesis has been provided in particular by observations that the toxicity induced *in vitro* by the HIV-1 envelope protein, gp120, requires the presence of microglia and/or macrophages (Lipton, 1992); and, the severity of AIDS-related neurologic disease correlates closely with the density of activated microglia and macrophages within the parenchyma (Glass *et al*, 1995).

The close relationship between the parenchymal density of activated microglia/macrophages and neurologic status has raised questions about the mechanisms by which this cell population may expand within the CNS. Previous studies have shown that either immune-activated or HIV-1-infected monocytes may traverse *in vitro* models of the blood–brain barrier (BBB) (Persidsky *et al*, 1997; Weiss *et al*, 1999) and that this recruitment may be regulated by the expression of specific adhesion molecules (Lafrenie *et al*, 1996; Nottet *et al*, 1996) and chemokines (Conant *et al*, 1998; Weiss *et al*, 1999). Indeed, trafficking of peripheral immune cells has been proposed to occur in a number of neurodegenerative disorders, and it appears likely that a similar cell migration may account in part for the accumulation of mononuclear phagocytes typically detected within the brains of lentivirus-infected hosts (Rausch *et al*, 1994; Glass *et al*, 1995; Gray *et al*, 1996). In contrast, relatively little attention has been paid to the possibility that local microglia and macrophage proliferation could contribute to the tissue burden of these cells. We have recently reported that microglia can be induced to proliferate *in vitro* following exposure to the feline immunodeficiency virus (FIV) (Meeker *et al*, 1999a), a lymphotropic and neurotropic lentivirus frequently used as a model for AIDS-related CNS disease (Meeker *et al*, 1997; Podell *et al*, 1999; Steigerwald *et al*, 1999). If this capability is retained *in vivo*, proliferation could play a significant role in the expansion of microglial and macrophage populations within the CNS.

An additional source of macrophages that may contribute to the brain macrophage burden may be the choroid plexus, a specialized invagination of the ventricular ependyma that provides a barrier between the peripheral circulation and the cerebrospinal fluid (CSF). Neuropathological studies have identified infected macrophages and possibly dendritic cells within the choroid plexus of HIV-1-infected patients (Falangola *et al*, 1995; Hanly and Petito, 1998; Petito *et al*, 1999), SIV-infected nonhuman primates (Lackner *et al*, 1991; Lane *et al*, 1996), and FIV-infected cats (Beebe *et al*, 1994). These studies have also noted that the choroid plexus stroma of lentivirus-infected hosts frequently contains an increased number of macrophages as well as infiltrating T-lymphocytes (Czub *et al*, 1996; Dean *et al*, 1993; Falangola *et al*, 1995; Hanly and Petito, 1998). These observations have raised the possibility that the choroid plexus could represent an important site of viral replication, release of macrophage-derived toxins, and trafficking of peripheral immune cells into the CSF. Yet, the extent to which the choroid plexus might contribute to AIDS-related neuropathogenesis *in vivo* is currently unclear, due largely to the fact that the interactions between lentiviruses and the cellular components of the choroid plexus have not been well characterized.

We have recently established primary cultures of feline choroid plexus to characterize the kinetics of lentiviral replication *in vitro*. We noted in these experiments that choroid plexus cultures exposed to FIV experienced an apparent increase in the number of macrophages, even though these cells typically reproduce poorly *in vitro*. This observation led us to question whether the increased macrophage density frequently detected within the choroid plexus of infected hosts could be due, at least in part, to local proliferation stimulated by lentiviral exposure. We have also hypothesized that interactions between choroid plexus macrophages and T-lymphocytes could result in an increased macrophage proliferation because 1) T-lymphocytes frequently infiltrate the choroid plexus during lentiviral infection; and 2) the activation of mononuclear phagocytes may be induced by exposure to CD40-ligand, a glycoprotein expressed on the surface of activated T-lymphocytes (Armitage *et al*, 1993; Caux *et al*, 1994; Kornbluth *et al*, 2000). Thus, in the present study we used multiple labeling techniques to evaluate the proliferation of choroid plexus macrophages following exposure to either FIV or rhuCD40L. In addition, we have also characterized the ability of FIV to promote the release of soluble neurotoxic factors in the choroid plexus culture supernatants. Our results indicate that either FIV or rhuCD40-ligand may stimulate choroid plexus macrophage proliferation *in vitro* and that this proliferation correlates closely with an increasing toxic activity detected in the cell culture supernatants.

Results

A representative example of the feline choroid plexus macrophage cultures is shown in Figure 1A. After 8 days *in vitro*, choroid plexus cultures consisted predominantly of a heterogeneous population of

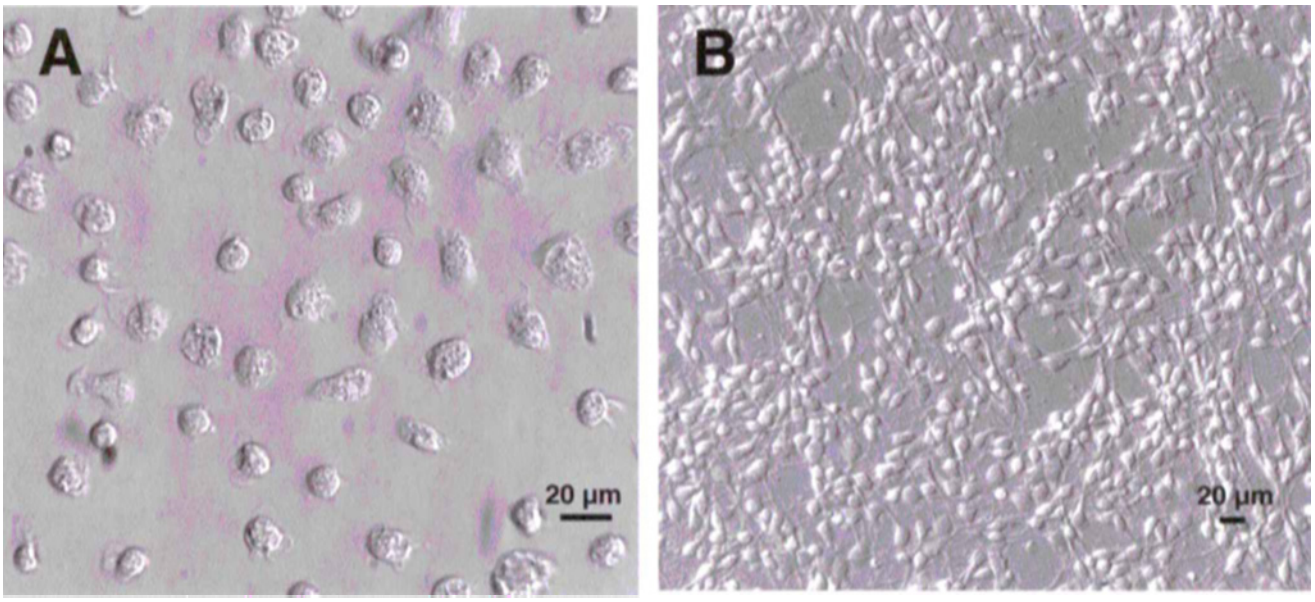

Figure 1 Primary cultures of feline choroid plexus macrophages and cortical neurons. (**A**) Example of untreated choroid plexus cultures enriched in macrophages with multiple phenotypes prior to inoculation with FIV. (**B**) Example of dissociated neurons used for toxicity analysis of macrophage-conditioned medium.

macrophages which displayed multiple phenotypes, including large, flattened cells as well as smaller, activated cells containing vacuoles and cytoplasmic processes. These cultures were used for the proliferation studies as well as for the production of supernatant for the assessment of neurotoxicity in cultures of feline cortical neurons (Figure 1B).

Accumulation of choroid plexus macrophages in vitro in response to FIV and rhCD40-L

Figure 2 shows the rate at which macrophages accumulated in choroid plexus cultures inoculated with FIV-NCSU at different viral doses or a virus-free ultrafiltrate. Cell counts obtained in each culture at days 3 and 6 postinoculation were expressed as increases relative to the corresponding baseline values, and the mean proportional increases were analyzed by Student's *t*-test. At day 3, a significant increase in macrophage accumulation was detected in choroid plexus cultures inoculated with either 10^4 ($P = 0.0178$; $n = 6$) or 10^5 ($P = 0.0314$; $n = 6$) $TCID_{50}$ FIV-NCSU compared to control cultures. At day 6, a significant increase was also observed in the cultures treated with 10^4 $TCID_{50}$ ($P = 0.034$; $n = 6$). However, the proportional increase in macrophage number in cultures inoculated with 10^5 $TCID_{50}$ of virus no longer represented a significant difference versus control cultures ($P = 0.113$; $n = 6$) due to an increased variability observed at this timepoint. Visual inspection of the cultures suggested that some macrophages may detach from the substrate after exposure to FIV and may be lost from the analysis over time. Choroid plexus cultures inoculated with 10^3 $TCID_{50}$ exhibited only slight changes in total macrophage number that were indistinguishable from the profiles observed in control cultures.

Macrophages in choroid plexus cultures inoculated with different concentrations of FIV-NCSU or ultrafiltrate were labeled by uptake of BrDU and fluorescent microspheres at 6 days postinoculation. An example of BrDU-positive nuclei within a cluster of unlabeled macrophages is seen in Figure 3A. At higher magnification the staining of the nucleus and

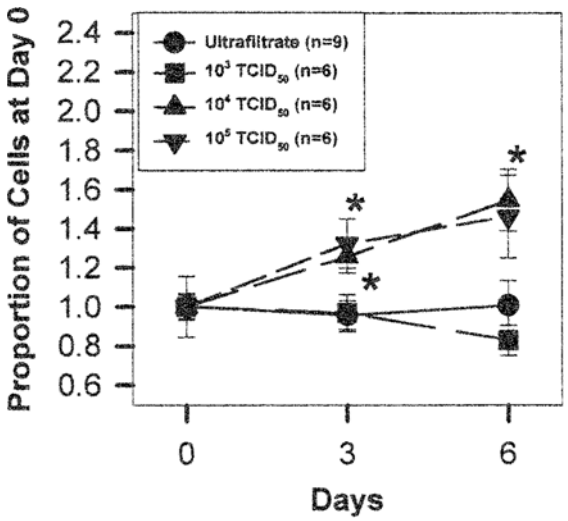

Figure 2 Proportional increases in macrophage accumulation in choroid plexus cultures relative to starting densities. Cultures were matched for initial macrophage density prior to inoculation with FIV or virus-free ultrafiltrate from the 10^5 $TCID_{50}$ stock. Cultures inoculated with either virus-free ultrafiltrate or 10^3 $TCID_{50}$ FIV-NCSU showed negligible increases above baseline values. Cultures inoculated with either 10^4 or 10^5 $TCID_{50}$ FIV-NCSU exhibited a marked accumulation of macrophages at days 3 and 6 postinoculation.

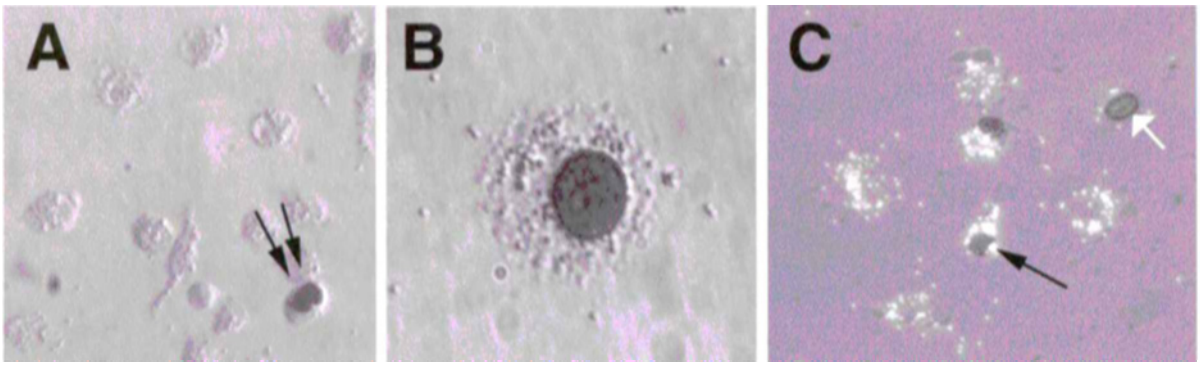

Figure 3 Choroid plexus macrophages inoculated with FIV and labeled with BrDU (3 days) and fluorescent latex microspheres (1 h). (**A**) BrDU-positive cells with darkly labeled nuclei can be seen within a cluster of choroid plexus macrophages. (**B**) BrDU-positive macrophage containing phagocytosed microspheres. (**C**) Combined brightfield and fluorescence illustrating BrdU staining within macrophages with a high density of microspheres (black arrow) and a BrdU-positive cell with no accumulation of microspheres (white arrow, nonmacrophage).

the abundant accumulation of microspheres is readily apparent (Figure 3B). Using combined brightfield and fluoresence optics, BrdU-positive macrophages filled with fluorescent latex beads (Figure 3C, black arrow) could be distinguished from BrdU-positive cells that exhibited minimal accumulation of latex beads (Figure 3C, white arrow). Similar results were obtained using green tyramide-enhanced immunofluorescence in combination with the red fluorescent latex beads (not shown). A significant increase in the percentage of BrDU-positive macrophages was observed in choroid plexus cultures inoculated with 10^3 $TCID_{50}$ ($P = 0.017$; $n = 3$) and 10^4 $TCID_{50}$ ($P = 0.0208$; $n = 3$) FIV-NCSU relative to control cultures (Figure 4). No significant difference was detected in cultures inoculated with 10^5 $TCID_{50}$ FIV-NCSU. Cell death was determined by staining parallel cultures with ethidium. The percentage of dead cells in the cultures was very low and did not vary significantly across conditions, ranging from 0.3%–0.6%. Because this corresponds to 0.6–2.0 dead cells/mm^2, it is clear that differential cell death does not contribute to the increases in the macrophages (25–85 new cells/mm^2).

Addition of rhuCD40-L to the cultured macrophages resulted in a dramatic, accelerating increase in the number of macrophages (Figure 5). Starting at densities of 59.2 and 54.0 cells/mm^2 for control and rhuCD40-L-treated cultures, respectively, the curves gradually began to separate. By day 6, the density of rhuCD40-L-treated macrophages was significantly greater than controls ($P = 0.045$, Mann–Whitney). By 12 days after treatment, the average density increased to 83.5 cells/mm^2 (3.4% day^{-1}) for controls and 434.4 cells/mm^2 (58.6% day^{-1}) for the rhuCD40-L-treated cultures, a 17-fold increase in the rate of

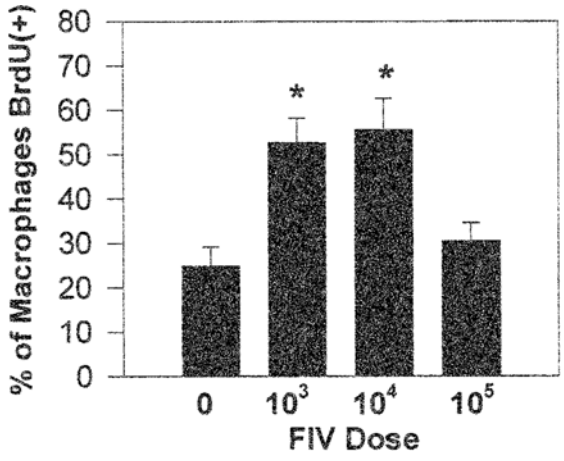

Figure 4 Increase in relative density of BrdU-immunoreactive macrophages after inoculation of choroid plexus cultures with 10^3 to 10^5 $TCID_{50}$ FIV-NCSU. Significant increases were seen in the cultures inoculated with 10^3 and 10^4 $TCID_{50}$. $^*P < 0.05$, FIV versus control.

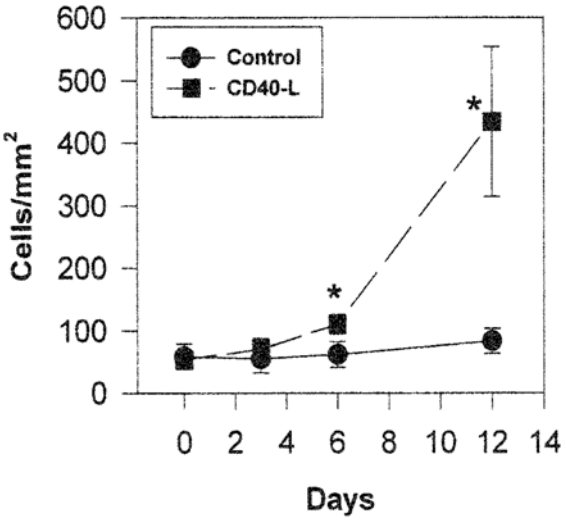

Figure 5 Proliferation of choroid plexus macrophages after exposure to 200 ng/ml rhuCD40-ligand trimer. rhuCD40-L was added to the culture medium at day 0. Cells were fed every 3 days with normal medium without rhuCD40-L and counted at days 3, 6, and 12. The growth curves showed a significant 77% increase over the controls by day 6, which expanded to a fivefold increase by 12 days. No significant increase in macrophages was seen in the control cultures over the 12 day period. Values represent the mean ± sem. $^*P < 0.05$ rhuCD40-L versus control.

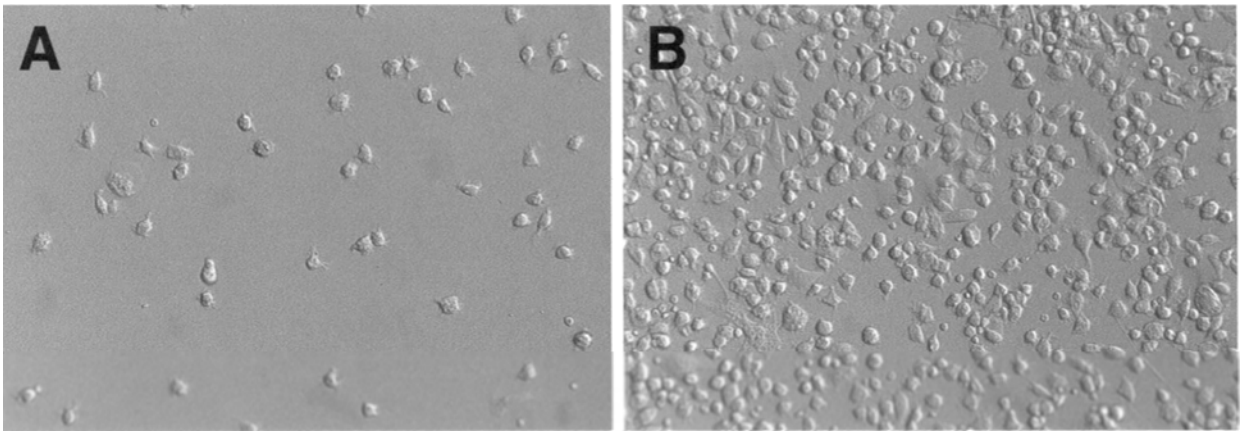

Figure 6 Example of the high density of choroid plexus macrophages often seen in culture 12 days after a single treatment with rhuCD40-L. (**A**) Density of choroid plexus macrophages seen in control cultures after 12 days. (**B**) High density of choroid plexus macrophages achieved in cultures treated with rhuCD40-L.

proliferation ($P = 0.006$, Mann–Whitney). As illustrated in Figure 6, some cultures reached extremely high densities of macrophages (Figure 6B) relative to matched controls (Figure 6A).

Toxic activity of choroid plexus-conditioned medium and feline CSF

Dissociated cultures of feline cortical neurons (e.g., Figure 1B) were exposed to either choroid plexus-conditioned medium or feline CSF and cell death was quantified by staining with ethidium homodimer. An increase in the number of dead cell nuclei was seen in the cultures treated with conditioned medium from FIV-infected macrophages relative to the small amount of cell death in the control cultures (conditioned medium in the absence of infectious FIV). In Figure 7, the average level of cell death produced by conditioned medium was expressed relative to the amount produced by the corresponding pre-inoculation medium. A proportional increase in toxic activity was detected in choroid plexus-conditioned medium following inoculation with FIV, whereas cultures inoculated with boiled virus showed no similar increase (not shown). Linear regression analysis of the rate of macrophage proliferation versus the increase in toxic activity in the culture supernatant over time (3, 6, and 9 days) following inoculation with FIV revealed a strong positive relationship ($r = 0.985$).

A similar increase in toxic activity was detected in CSF from cats infected with FIV. CSF collected at 16 weeks' postinoculation produced a significant increase ($P = 0.018$; $n = 6$) in the level of cell death relative to the amount produced by CSF collected prior to inoculation (Figure 8). In addition to the early CSF samples, CSF collected from four cats at 1 year postinfection was tested and showed even higher levels of toxic activity in three of the four cats suggesting a progressive increase in the release of putative toxins over time. These cats exhibited a significant CSF viral load (Figure 9) and a decrease in cortical *N*-acetylasparty l glutamate (NAA) content (Figure 10). The CSF viremia generally paralleled the plasma viremia, peaking at 3 weeks postinoculation and decreasing thereafter to low levels (Figure 9). In contrast, toxic activity increased while the CSF and plasma viremia decreased. The decrease in CSF FIV was slower than the decrease in plasma FIV after the early peak viremia resulting in a substantial, 259-fold, decrease in the mean plasma:CSF FIV ratio from 1088 at the peak to 4.2 at 18 weeks. During this time, none of the animals showed clinical neurologic signs on standard veterinary neurologic examination (including cognitive and behavioral assessment). A sensitive measure of tissue NAA levels using HPLC

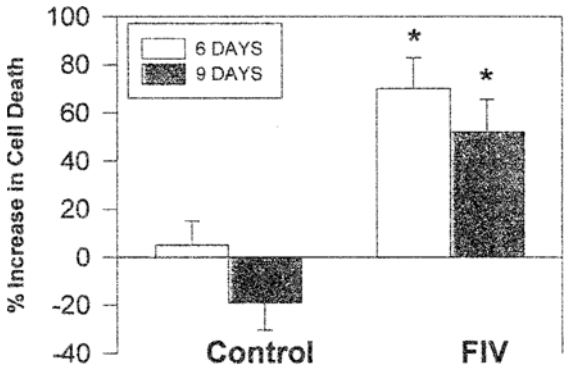

Figure 7 Toxicity induced in dissociated cortical cultures by conditioned medium collected from choroid plexus cultures inoculated with FIV. Dissociated cultures were incubated for 24 h in choroid plexus-conditioned medium, and cell death was quantified by staining with ethidium homodimer. The mean (± s.e.m.) cell death produced by samples collected at days 6 and 9 postinoculation were expressed relative to the amount produced by conditioned medium collected at baseline (pre-inoculation). Choroid plexus cultures inoculated with FIV exhibited an increasing toxic activity in the culture supernatants, reflected by an increase in the relative amount of cell death induced in dissociated neural cultures. Control choroid plexus cultures inoculated with boiled FIV showed no similar increase. $^*P < 0.01$, $n = 8$ wells/condition.

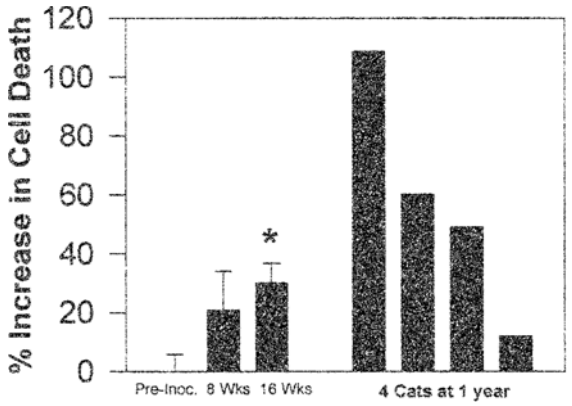

Figure 8 Toxicity produced in feline dissociated cultures by CSF collected from cats experimentally infected with FIV. CSF was ultrafiltered at a MWCO of 100 kDa and was added to the culture medium at a dilution of 1:20. CSF collected at 16 weeks postinfection produced a significant proportional increase in cell death relative to the pre-inoculation sample.

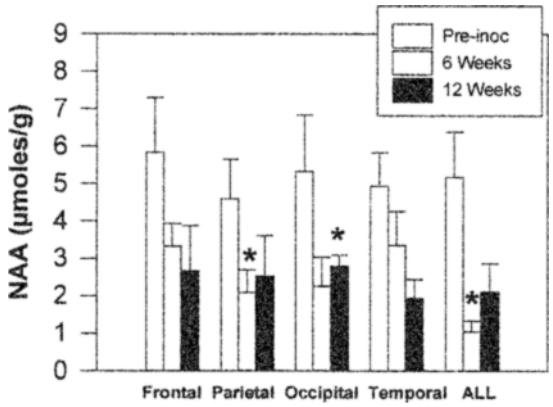

Figure 10 *N*-acetylaspartylglutamate levels in cortical tissue of cats infected with NCSU-FIV by intravenous inoculation. Tissue is from the same cats used as donors of CSF for the toxicity and viremia measures illustrated in Figures 8 and 9. Whole brain values reflect the mean of individual lobes. NAA was significantly decreased ($P < 0.05$, Mann–Whitney test) at 6 weeks post infection in the parietal lobe and whole brain and in the occipital lobe at 12 weeks post infection.

revealed uniform decreases in cortical content by 6 weeks postinfection (Figure 10). Analysis of individual cortical regions showed significant reductions in NAA within the parietal lobe at 6 weeks and the occipital lobe at 12 weeks.

CD18 and MAC387 immunoreactivity in vivo

Robust CD18 immunoreactivity was detected in the choroid plexus stroma and periventricular regions in cats infected experimentally with FIV-NCSU (Figure 11B), whereas stained cells were lighter and more sparse in the corresponding regions in sham-inoculated control cats (Figure 11A). The pattern of immunoreactivity was characterized by a staining gradient that was most intense along the ependymal surface of the ventricular wall and decreased with penetration into the parenchyma. Close inspection revealed a high density of immunoreactivity between and along the parenchymal surface of the ventricular ependymal cells (Figure 11C). Immunohistochemical staining with an antibody specific for feline monocytes/macrophages (MAC387) revealed a slightly different pattern, summarized in Figure 12. The choroid plexus of uninfected cats showed low or negligible staining and the corresponding brain tissue surrounding the ventricles showed occasional weak immunoreactivity associated with blood vessels or rare cellular staining. FIV-infected cats with AIDS showed stronger immunoreactivity in the choroid plexus as well as in the surrounding brain tissue. Cells were occasionally observed to have long immunoreactive processes. Immunoreactivity in the brain was not concentrated in the region of the ventricles, as with the CD18 stain. Immunoreactive cells were seen throughout the cortex of FIV-infected cats. Staining intensity correlated with the level of infection. Uninfected cats had negligible staining, FIV-infected, non-AIDS cats intermediate levels of staining and AIDS cats the greatest amount of staining. Abundant immunoreactivity was seen associated with blood vessels in the cortex of the AIDS cats. Numerous round immunoreactive cells were also seen near the cortical surface of the AIDS cats. Immunoreactive cells in the cortex occasionally showed long processes, often associated with blood vessels. These observations support a progressive and widespread increase in macrophage infiltration in the brain during FIV infection.

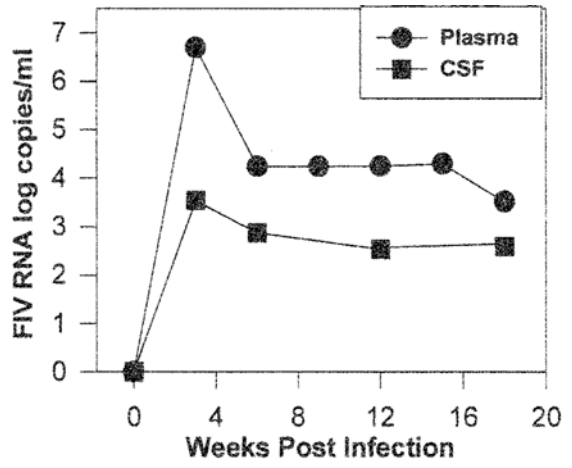

Figure 9 Temporal profile of plasma and CSF viremia in four cats infected with NCSU-FIV by intravenous inoculation. Viral titers were highly variable between cats but consistently showed the same temporal pattern. CSF collected at 0, 6, and 18 weeks from these cats was used for toxicity analysis.

Discussion

The mononuclear phagocytes of the choroid plexus have been divided into subpopulations based primarily on anatomical distribution and immunophenotype, although clear functional distinctions have not yet been made. Epiplexus cells, first described by

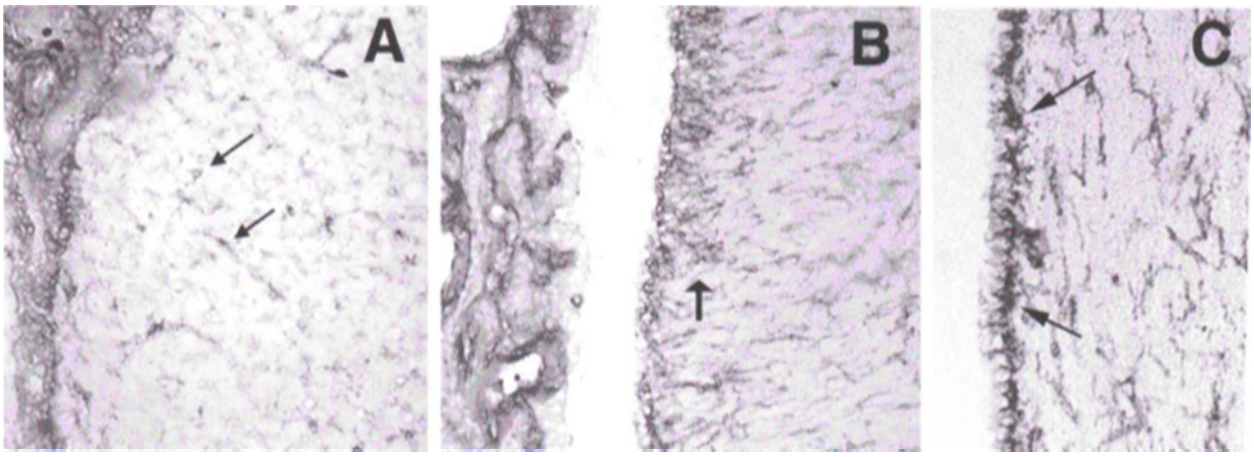

Figure 11 CD18 immunoreactivity in cats infected experimentally with FIV versus sham-inoculated control cats. Light staining of scattered microglia-like cells (arrows) is observed in periventricular regions in control cats (**A**), in contrast to a more robust labeling seen in the corresponding regions in FIV-inoculated cats (**B**). In the FIV-infected cats, a staining gradient is apparent with the highest density adjacent to the ependymal cell layer of the ventricle (arrow). At higher magnification (**C**), robust labeling of cells is seen between and adjacent to the ependymal cells (arrows).

Kolmer, have been typically observed in close association with the choroidal epithelium (Ling *et al*, 1998), while macrophages may be distributed throughout the stroma (Matyszak *et al*, 1992). More recent studies indicate that the choroid plexus may also contain an intrinsic population of dendritic cells (DCs), distinguished by a characteristic stellate morphology and expression of DC-specific surface antigens (Matyszak and Perry, 1996; Serot *et al*, 1997; Hanly and Petito, 1998; McMenamin, 1999). Developmental studies have suggested that choroid plexus macrophages and epiplexus cells both represent bone marrow-derived elements that differentiate from circulating monocytes (Ling, 1979), and it is likely that the putative choroid plexus DCs are similarly derived based on studies of other DC populations (Banchereau and Steinman, 1998). Yet relatively few studies have characterized the normal turnover of these cells or the mechanisms underlying the accumulation that may occur in response to various inflammatory stimuli. Although there have been reports that stromal macrophages and epiplexus cells may proliferate (Matyszak *et al*, 1992; Lu *et al*, 1993), the number of dividing cells observed in both experiments constituted only a small percentage of the total population. It is therefore possible that the density of mononuclear phagocytes in the choroid plexus may be maintained by a combination of mechanisms, including local proliferation and recruitment of peripheral precursor cells.

In the present study we examined the effects of FIV on primary cultures of feline choroid plexus, which consisted predominantly of a heterogeneous population of mononuclear phagocytes. In this report we have collectively referred to these cells as macrophages in the absence of surface markers that may distinguish particular subpopulations *in vitro*. The data indicate that choroid plexus cultures exposed to FIV experience an increased rate of macrophage accumulation relative to control cultures. Comparison of the relative levels of proliferation and cell death further confirmed that this accumulation represented an increased rate of replication, as the extent of cell death was very low and did not vary between cultures treated with either virus or virus-free ultrafiltrate. We have previously shown that feline microglia in mixed neural cultures exhibit an increase in proliferation following an *in vitro* challenge with FIV (Meeker *et al*, 1999a). Although the dose-response relationships observed for FIV-induced increases in microglia and macrophage proliferation were strikingly similar, the rates of replication were significantly different. Following exposure to FIV, the rate of microglial proliferation increased to an average of 40% day^{-1}, in contrast to a maximum rate of 20% day^{-1} observed for choroid plexus macrophages. Moreover, the effects of FIV on microglial proliferation were dependent on soluble factors released from astrocytes and/or neurons, neither of which was present in choroid plexus cultures. However, we have not examined whether the presence of small numbers of contaminating fibroblasts and epithelium may influence the observed effects on macrophage proliferation.

The use of fetal cultures allowed parallel cultures of choroid plexus and neurons in our studies. However, it should be noted that these macrophages are cultured at a time when they are typically proliferating *in vivo*. Although these cells appear to differentiate into a mature and active phenotype in culture it is important to note that they may retain a greater proliferative capacity than choroid plexus macrophages in adults. This is something that will need to be examined further since it could be a significant variable associated with disease progression in the immature brain.

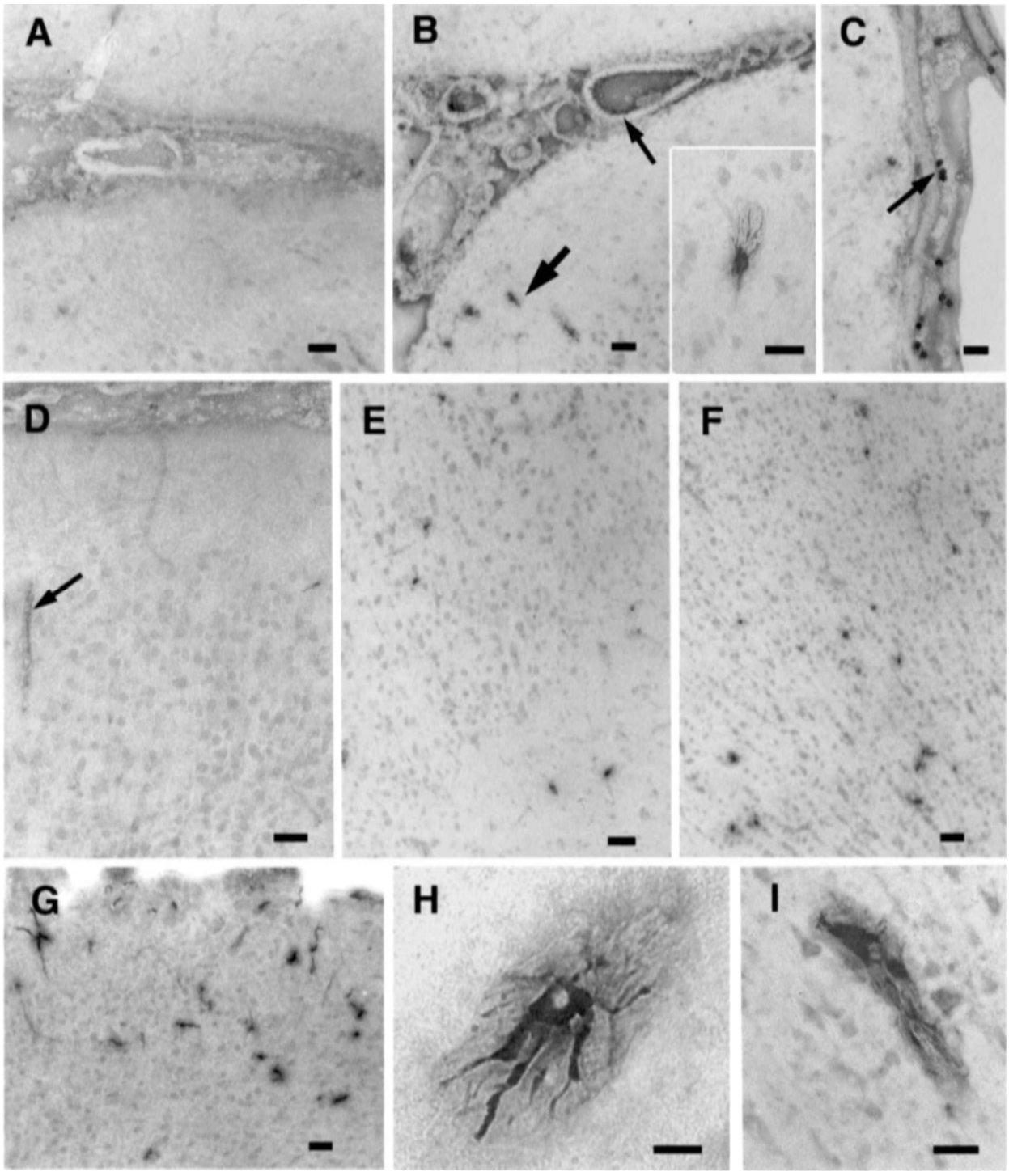

Figure 12 MAC387 immunoreactivity in FIV-infected cats. The macrophage specific antibody, MAC387, produced very little staining in the brain of uninfected cats. (**A**) Regions in and around the choroid plexus occasionally showed very light immunoreactivity. (**B**) FIV-infected cats with AIDS showed heavier immunoreactivity within the choroid plexus (small arrow), particularly in the region along the basal surface of the epithelium. Heavily stained cells or clusters of cells could be seen in the adjacent parenchyma (large arrow). These cells occasionally displayed long processes (inset). (**C**) Heavily immunostained cells were also visible within the meninges of the AIDS cats over the surface of the cortex. Stained cells were also seen throughout the cortex. (**D**) Weak staining was occasionally seen in the cortex of uninfected cats, often associated with the vasculature (arrow). (**E**) Immunoreactive cells were seen in the brains of asymptomatic FIV-infected cats. (**F**) FIV-infected cats with AIDS had greater numbers of immunoreactive cells throughout the cortex. (**G**) Staining in the AIDS cats was also very prominent within the vasculature near the surface of the cortex. (**H**) Clusters of strongly immunoreactive cells with long processes in the cortex of an AIDS cat. (**I**) Immunostained processes often appeared to follow the vascular endothelium. Bars: 25 μm.

A more dramatic increase in macrophage proliferation was observed in choroid plexus cultures exposed to rhuCD40-L, a member of the tumor necrosis factor (TNF) superfamily which is expressed on the surface of activated T-lymphocytes (Armitage *et al*, 1993). Previous studies have shown that interactions of CD40-ligand (CD40L) with its receptor, CD40, promotes the activation and survival of dendritic cells (Caux *et al*, 1994). Recent studies have further suggested that a wide range of mononuclear phagocyte effector functions may be modulated by the CD40/CD40L system and that these signal transduction events could be particularly important for the replication of HIV-1 (for review, see Kornbluth *et al*, 2000). Results from the present study demonstrate that CD40L may induce a significant increase in macrophage proliferation, suggesting that T-cells trafficking into the choroid plexus could provide a more potent stimulus for proliferation than exposure to lentivirus.

In addition to the effects on macrophage proliferation, FIV induced the release of a soluble factor(s) that produced significant toxicity in feline cortical cultures. Furthermore, there was a significant positive correlation between macrophage proliferation and toxic activity in the culture supernatants, indicating that, among the multiple cell types present *in vitro*, choroid plexus macrophages represented the major effector cells driving toxicity. Although the choroid plexus-derived factor(s) has not been identified, previous studies of microglia suggest several possibilities. There is considerable evidence that lentiviral exposure may induce macrophages/microglia to release a number of putative neurotoxins, including tumor necrosis factor-α (TNF-α) (Sopper *et al*, 1996; Wesselingh *et al*, 1997; Poli *et al*, 1999), interleukin-6 (Yeung *et al*, 1995; Sopper *et al*, 1996), quinolinate (Heyes *et al*, 1998), platelet-activating factor (Gelbard *et al*, 1994), nitric oxide (Adamson *et al*, 1996), and a novel, partially characterized toxin, NTox (Giulian *et al*, 1996). Neurotoxicity may also be induced by the viral regulatory protein, tat (Magnuson *et al*, 1995) and the surface glycoprotein, gp120 (for review, see Nath and Geiger, 1998). Although we have previously shown that FIV may achieve a low grade productive infection in choroid plexus macrophages (unpublished observations) and that the FIV envelope protein induces excitotoxicity in neural cultures (Bragg *et al*, 1999), the effects produced by choroid plexus-conditioned medium cannot be atttributed to either virus or envelope protein because both would be excluded by filtration of the culture supernatant. Thus the size restrictions imposed by filtration reveal that the putative neurotoxin derived from choroid plexus must be a factor of a molecular weight less than 100000.

Because the choroid plexus manufactures the bulk of the cerebrospinal fluid (CSF) that fills the ventricles, subarachnoid space, and spinal canal (Johanson *et al*, 1999), it is possible that toxic factors produced within this structure could be released into the CSF and diffusely distributed throughout the CNS. Previous studies have demonstrated that a number of the diffusible factors implicated in AIDS-related neurotoxicity have indeed been detected within the CSF of HIV-1-infected patients [for review, see Bragg *et al* (2000)]. Moreover, we recently reported that CSF collected from HIV+ individuals contains a low molecular weight factor that promotes toxicity in primary neural cultures (Meeker *et al*, 1999b). In the present study we performed a similar analysis on CSF collected from cats infected acutely with FIV and directly compared this profile to the effects produced by supernatants harvested from FIV+ choroid plexus cultures. Within weeks of experimental infection with FIV, a significant toxic activity is detected in CSF that resembles the profile previously reported for CSF from HIV-1-infected patients. The relationship between the appearance of the toxic factor and the plasma and CSF viremia was inverse, as the toxic activity increased while the CSF and plasma viremia decreased. This suggests that once the CNS inflammatory process is initiated, it may not be tightly linked to CSF viral load. Alternatively, the appearance of toxic factors could reflect the development of a primary infection of brain tissue that is only partially represented in the total CSF virus. The tendency for the CSF:plasma FIV ratio to reverse is consistent with this possibility. The origins of toxic factors detected in CSF during lentiviral infection are still unclear, and it is likely that they may derive from multiple sources within the CNS and periphery. However, the similarities between the toxic profiles produced by FIV+ choroid plexus culture supernatants and FIV+ CSF raise the possibility that the choroid plexus could make an important contribution to pool of toxic factors circulating within the CSF/ventricular system.

We also observed an increased immunoreactivity for CD18 in periventricular regions in FIV-infected versus sham-inoculated control cats. The most intense staining was observed in regions that lie closest to the choroid plexus, with a gradient of staining intensity that decreased with deeper penetration into the parenchyma. Although this increased immunoreactivity could reflect either an increased number of monocytic cells or level of CD18 expression, the pattern is particularly suggestive of cells trafficking from the choroid plexus. A high level of choroid plexus macrophage proliferation could support such a process. In addition, the potential for trafficking of systemic monocytes is indicated indirectly by observations of: 1) inflammatory infiltrates in the choroid plexus of lentivirus-infected hosts (Beebe *et al*, 1994; Falangola *et al*, 1995; Czub *et al*, 1996; Hanly and Petito, 1998); 2) increased mononuclear cells frequently detected in CSF during the early stages of HIV-1 infection (McArthur *et al*, 1989; Martin *et al*, 1998; Gisslen *et al*, 1999); and 3) increased adhesion molecule expression on the choroid plexus epithelium during CNS inflammation

(Steffen *et al*, 1996; Wolburg *et al*, 1999). Staining with MAC387, which detects feline macrophages but not microglia, confirmed increased immunoreactivity in and around the choroid plexus but failed to show the same pattern of staining within the ependymal cell lining. Instead, the increases in immunoreactivity in the AIDS cats were widespread and included heavy staining associated with the vasculature and cells over surface of the cortex. However, it is important to note that the stromal macrophages of the choroid plexus were not stained by the MAC387 antibody as evidenced by the lack of staining in the control cats and the relatively discrete staining patterns in the FIV-infected cats. Thus, while the observations support a widespread and diffuse penetration of monocytic cells through the choroid plexus and vasculature questions still remain regarding the precise role of the choroid plexus macrophages which may represent a unique, expanding population of cells that contribute to toxic inflammatory interactions in subcortical regions known to be targeted by HIV-1 (Navia *et al*, 1986).

Materials and methods

Experimental animals

Ten specific pathogen-free (SPF) cats were obtained from Liberty Labs (Liberty Corner, NJ), maintained and bred at the North Carolina State University College of Veterinary Medicine (NCSU-CVM). Additional fetal tissue was obtained from random source cats during spaying and neutering of the cats by a nonprofit population control program. The cats within a treatment condition were gang housed and fed a commercial diet in AAALAC-accredited facilities. After arrival and acclimation, each cat received a physical and neurological examinations and was screened for FIV antibody by commercial ELISA (IDEXX). All cats were negative for FIV.

Primary cultures of brain and choroid plexus

Fetuses were removed by cesarean section or by removal of the uterus during routine spaying at approximately 25–40 days gestation. Brains were removed from the cranium and rinsed 3× in fresh sterile HEPES-buffered Hanks' balanced salt solution (HBSS in mM: NaCl, 138.0; KCl, 5.36; $CaCl_2$, 1.26; $MgSO_4$, 0.40; $MgCl_2 \cdot 6H_2O$, D-glucose, 5.55; HEPES, 20; pH to 7.4 with NaOH).

Choroid plexus cultures The choroid plexus was dissected from the cerebral ventricles and rinsed 3× in HBSS. Pooled tissue explants were minced with sterile forceps, and the resulting cell suspension seeded uniformly onto poly-D-lysine-coated (0.1 mg/ml) glass coverslips in each well of a 24-well plate under a thin layer of medium. Cells were maintained in a 5% CO_2 incubator at 35–36°C and fed every 3 days with Dulbecco's Modified Eagle Medium (DMEM), supplemented with 10% FBS and 20 μg/ml gentamicin (complete medium). After 8 days *in vitro*, the choroid plexus explant had detached and remained in suspension. Coverslips were enriched in macrophages at densities ranging from approximately 50–170 cells/mm^2, with some fibroblasts and endothelial cells present as well. Under these conditions, choroid plexus epithelial cells and endothelial cells did not attach to the substrate and were typically depleted during exchange of the culture medium. Only small amounts of epithelium remained *in vitro* by the end of the first week in culture. The relative purity of the macrophages at the initiation of the experiments was 92 ± 4% .

Dissociated cultures of feline cortex Cortex was dissociated to provide mixed cultures of uniform density for the analysis of the toxicity of choroid plexus macrophage conditioned medium. The cerebral hemispheres were dissected from the fetal brain, minced, and incubated in 5 ml calcium/magnesium-free-HBSS containing 2.5 U/ml dispase +2 U/ml DNase I for 10 min at 37°C. The tissue was triturated by 10 passes through a 10-ml pipette. Undissociated tissue clumps were allowed to settle for 2 min, and suspended cells were transferred to a culture tube containing 25 ml complete medium. The remaining tissue was resuspended in 5 ml HBSS and again triturated for 10 passages through a 10-ml pipette. The pieces were allowed to settle, cells collected, and the procedure repeated until most tissue was completely dispersed. The cells were seeded at a density 10^5 cells/cm^2 in each well of a 48-well plate. The resulting cultures, at the time of testing, contained a mixed population of cells predominantly consisting of neurons, astrocytes, and small numbers of microglia.

Source of FIV

All studies used an infectious molecular clone of the FIV-$NCSU_1$ isolate (FIV-$NCSU_1$) prepared as previously described (Yang *et al*, 1996). The FIV-$NCSU_1$ clone was propagated in an interleukin-2-dependent feline CD4+ T-lymphocyte cell line, FCD4-E (English *et al*, 1993). Virus grown in FCD4-E cells was harvested, centrifuged, filtered through a 0.2-μm filter and maintained as a cell-free stock at a concentration of approximately 10^8 tissue culture infectious $doses_{50}$ ($TCID_{50}$)/ml.

Inoculation with FIV

Choroid plexus cultures were stimulated *in vitro* with concentrations of FIV ranging from 10^2 to 10^5 $TCID_{50}$/ml. After 48 h, cells were washed 3× in HBSS, and fed with complete medium. Control cultures were challenged with either boiled virus, prepared by incubating the virus stock at 100°C for 20 min, or a virus-free ultrafiltrate, prepared by passing the viral stock through a 100000 M.W. cutoff filter.

Specific pathogen-free (SPF) cats, ranging in age from 6 to 12 months, were injected intravenously with 2×10^6 $TCID_{50}$ FIV-$NCSU_1$ in 100 μl of

cell-free culture supernatant. Control cats were sham-inoculated with vehicle (culture medium). Infection was confirmed by the presence of FIV-specific antibodies in plasma, measured by a commercial ELISA (Idexx Laboratories, Westbrook, ME), and FIV proviral DNA sequences in peripheral blood mononuclear cells (PBMCs), amplified by PCR as previously described (Meeker *et al*, 1996). All FIV-inoculated cats were antibody-positive and provirus-positive by 6 weeks postinfection.

Accumulation of choroid plexus macrophages in vitro

The number of macrophages present in choroid plexus cultures was determined by either visual inspection or digital morphometry. In both cases, cells were washed 3× and maintained in a HEPES-based artificial CSF (aCSF) for the duration of the procedure. Cells were viewed on an Olympus IMT-2 inverted microscope under Hoffmann optics in a defined field of 0.294 mm^2, with measurements systematically taken from three fields per well. For visual inspection, macrophages were identified and counted based on characteristic morphology. For digital morphometry, macrophages were first labeled by uptake of acetylated low density lipoprotein conjugated to the fluorescent dye, 1,1′-dioctadecyl-3,3,3′,3′-tetramethylindocarbocyanine (DiI-acyl-LDL; Biomedical Technologies; 2.0 μg/ml in DMEM at 37°C for 60 min). Under these conditions, macrophages were selectively stained at a very high signal-to-noise ratio. Digital images of each field were captured by a Metamorph Imaging System (Universal Imaging Corporation, West Chester, PA), and fluorescent cells were automatically highlighted and filtered based on size (μm^2) so that only objects consistent with macrophages were counted. This procedure also eliminated clusters of macrophages and although some care was taken to avoid clusters that could not easily be resolved, values may slightly underestimate proliferation. Other cell types including endothelial cells showed very weak or negligible staining and were easily distinguished from the macrophages.

To determine the rate of macrophage accumulation in choroid plexus cultures, macrophage density *in vitro* was measured prior to stimulation with either FIV or a virus-free ultrafiltrate or rhuCD40-ligand trimer, generously provided by Immunex Corporation. Cultures were then assigned to the experimental and control conditions to provide equivalent average starting densities. Cells were thoroughly washed 24 h after inoculation and counted again at days 3, 6, and 9 postinoculation. In some experiments the macrophage density became too high for automated counting requiring estimates obtained through manual counting.

The proliferation of choroid plexus macrophages was verified by uptake of bromodeoxyuridine (BrDU). Choroid plexus cultures inoculated with either FIV or virus-free ultrafiltrate were placed in complete medium containing 10 μM BrDU. After 3 days, cultures were incubated in a suspension of carboxylate-modified red fluorescent (580/605) microspheres (1-μm diameter; Molecular Probes; Eugene, OR), which are selectively taken up by phagocytic cells. After 1 hour cells were washed 3× with HBSS and fixed in Carnoy's Fluid (glacial acetic acid: chloroform: ethanol; 1:3:6 vol:vol:vol) or 4% paraformaldehyde in 0.01 M phosphate-buffered saline, pH 7.4. Fixed cells were rinsed in ice cold phosphate-buffered saline (PBS, 0.01 M, pH = 7.4) and permeabilized by a 5-min incubation in 2 N HCl. Coverslips were washed sequentially in ice cold deionized water and PBS, then incubated overnight in a mouse anti-BrDU antibody (6 μg/ml in 0.05 M Tris-buffered saline, pH = 7.6). On the following day, cultures were washed in PBS and incubated in biotinylated goat anti-mouse IgG for 1 hour. After washing cells in PBS, bound antibody was visualized by the ABC method (Vector Labs; Burlingame, CA) using diaminobenzidine (0.5 mg/ml in PBS with 0.01% H_2O_2). After rinsing in PBS, coverslips containing cells were dehydrated through a series of alcohols, cleared in xylene, and mounted on slides. Cells were examined by both fluorescence and light microscopy at a magnification of 400×. Choroid plexus macrophages were identified based on morphology and uptake of fluorescent microspheres, an indication of phagocytic activity. The number of BrDU-positive cells in this population was counted to determine the percentage of choroid plexus macrophages undergoing proliferation.

Cell death in choroid plexus cultures was determined by staining with ethidium homodimer (2 μM in DMEM for 40 min; Molecular Probes; Eugene, OR), which labels the nuclei of dead cells. Choroid plexus macrophages were labeled with fluorescent microspheres and in some cultures, BrdU as detailed previously prior to fixation for immunohistochemistry.

CD18 and MAC387 immunohistochemistry

Three SPF cats infected experimentally with FIV-$NCSU_1$ for 2 to 3 years and 3 age-matched sham-inoculated cats were anesthetized with a lethal dose of sodium pentobarbital. Brains were removed from each cat, transected along the midline, and snap-frozen in isopentane. Cryostat sections of 30-μm thickness were cut through blocks of frontal and parietal containing lateral ventricle with choroid plexus.

The density of microglia/macrophages within the choroid plexus and adjacent parenchyma was evaluated by immunohistochemistry for CD18. Fresh frozen sections were fixed in ice-cold methanol: acetone (1:1), washed 3× in PBS and incubated in 0.6% H_2O_2 in PBS for 15 min. Tissue was washed an additional 3× in PBS and incubated for 45 min in 3% normal goat serum. Primary antibody was applied

at a 1:500 dilution in 10% cat serum, 0.3% normal goat serum in 0.01 M PBS. After an overnight incubation at 4°C, the tissue was washed three times and incubated for 2 h in biotinylated goat anti-mouse IgG (Vector Labs, 1:200). After washing in PBS, the tissue was incubated in ABC reagent followed by reaction in 0.05 mg/ml diaminobenzidine +0.01% H_2O_2.

A similar procedure was followed for the MAC387 antibody based on the recommendations of the supplier (DAKO, Corp, Carpenteria, CA.). Briefly, tissue was rinsed with wash buffer (0.05 M Tris-HCl, 0.15 M NaCl, 0.1% Tween-20, pH = 7.6) and treated for 5 min with 3% H_2O_2. Sections were washed and incubated overnight at 4°C in primary mouse monoclonal anti-human myeloid/histiocyte antigen at a dilution of 1:100 in wash buffer. The sections were then washed and stained by the ABC method using the DAKO LSAB-2 kit with diaminobenzidine as substrate.

Collection of choroid plexus-conditioned medium and cerebrospinal fluid (CSF)

On day 2 after culture, rhuCD40-L was added to the medium for 24 h to stimulate the proliferation and differentiation of macrophages. The cells were fed normally on culture days 3 and 6. On day 8, the cultures were inoculated with 10^4 $TCID_{50}$ FIV. Conditioned medium was collected from choroid plexus cultures at days 0 (pre-inoculation), 6, and 9 postinoculation with FIV. Conditioned medium was passed through a 100,000 M.W. cutoff filter to remove virus and large proteins, then stored at −80° pending toxicity analysis. CSF was collected from the cerebromedullary cistern (cisterna magna) from FIV-inoculated and control cats at 0, 3, 6, 12, and 18 weeks and 1 year postinoculation.

Quantitative-competitive RT-PCR for analysis of FIV mRNA

A wild-type positive control plasmid (pCP1) and a competitive template (pCP1 + 169) were constructed. An Xba I/EcoR I fragment of the FIV-NCSU1 *gag* gene was cut from a pVL3-Wgag plasmid and ligated into pGEM-11Zf(+) transcriptional vector (Promega) multiple cloning site. A blunt ended pUC19 Dde I fragment (169 bp) was ligated into a blunt ended pCP1 at the Bfr I site and resulted in construction of pCP1 + 169. The pCP1 is identical to pCP1 + 169 except for a 169-bp fragment addition at the Bfr I site within *gag*. The insertion was confirmed by restriction analysis and PCR. *In vitro* transcription was performed by using T7 polymerase (Promega) according to manufacturer's directions. Transcripts were treated with RNase-free DNase (Promega). Phenol/chloroform extraction was performed twice and the RNA-containing fractions were selected on a Select D (RF) column (5′-3′, Boulder, CO), treated with proteinase K, extracted 3× with phenol/chloroform and precipitated with ethanol.

RNA from 0.2 ml of cell-free plasma or CSF was extracted using a single-step method with TRI-REAGENT (Molecular Research Center, Inc) according to the manufacturer's protocol. The resulting pellet was suspended in 40 μl of DEPC-treated water and used immediately for analysis. For reverse transcription with SuperScript II RNaseH$^-$ (Gibco BRL; according to manufacturer's protocol), 4 μl of plasma RNA solution was added to a series of 2-fold dilutions, ranging from 6250 copies/μl to 48 copies/μl, of pCP1 + 169 RNA template. The resulting cDNA was amplified with hot-start PCR at 99°C for 10 min followed by a 40-cycle program consisting of 3 cycles of 97°C for 1 min, 55°C for 2 min, 72°C for 1 min, and 37 cycles of 94°C for 1 min, 55°C for 2 min, 72°C for 1 min with an extension of 72°C for 10 min.

Primers were selected from the end of a major core region of FIV-14. The sense primer was located at 1518–1541 (5′ CCA AAT AGA TCA AGA ACA AAA TAC 3′) and the antisense primer was located at 1713–1693 (5′ AAG AGC TTC TGC CAA GAG TTG 3′). The RNA pellet was resuspended in DEPC-treated water and quantitated. Primers amplify a 196-bp product from the wild-type and a 365-bp competitor. Following amplification, reaction products were separated on a 3% TAE agarose gel containing ethidium bromide, photographed, and quantified using Adobe Photoshop and NIH Image software programs (Rottman *et al*, 1996). As a control for FIV provirus contamination, the same amount of RNA was PCR-amplified without reverse transcription. Levels of viral RNA in the CSF were also determined by qcRT-PCR using the protocols as described for plasma.

Neurotoxicity of choroid plexus-conditioned medium and CSF

Dissociated cultures of feline cortex were incubated in either choroid plexus-conditioned medium (1:1) or feline CSF diluted 1:20 in DMEM for 24 h. All samples were assayed in triplicate, and cortical cultures were pre-screened to verify equivalent initial cell densities. Cells were washed 3× in HBSS, and dead cell nuclei were labeled with ethidium homodimer (2 μM in DMEM, 40 min, 37°C). Cells were washed again and maintained in HBSS while fluorescent nuclei were automatically sized and counted. Digital images of fluorescent nuclei were captured by the Metamorph System and filtered based on size (μm^2), so that only objects in the appropriate size range were automatically counted. Five fields of 0.295 mm^2 at a magnification of 267× were measured per well, and the mean number of labeled nuclei per field was used to calculate the density of dead cells in each culture (dead cells/mm^2). Toxicity results were expressed as proportional increases relative to baseline: the cell death produced by conditioned medium or CSF collected at each postinoculation time point was divided by the amount produced by the corresponding

pre-inoculation sample. Basal cell death in cultures treated with an artificial CSF was also measured to control for normal cell death in the cultures.

Analysis of tissue N-*acetylaspartate (NAA) content*
Cortical brain tissue, 0.1–0.3 g, was added to 2 ml of 0.1 M $HClO_4$ and acetonitrile (1:1), homogenized, sonicated for 1 min, and centrifuged. The supernatant was transferred to a microseparation system equipped with 3000-Da molecular weight filter and centrifuged for 30 min at $3000 \times g$. The ultrafiltrate was then ready for HPLC determination.

The photodiode array detector was set at 200- to 300-nm range (l = 210 nm). The column utilized was an ODS-2 with 5-μm spheres, 4.6 × 150 mm. The column temperature was 40°C. The first mobile phase was 2% acetonitrile in 0.1 M phosphoric acid. The second mobile phase was 50% acetonitrile in 0.1 M phosphoric acid.

References

Achim CL, Wang R, Miners DK, Wiley CA (1994). Brain viral burden in HIV infection. *J Neuropathol Exp Neurol* **53:** 284–294.

Adamson DC, Wildemann B, Sasaki M, Glass JD, MacArthur JC, Christov VI, Dawson TM, Dawson VL (1996). Immunologic NO synthetase: elevation in severe AIDS dementia and induction by HIV-1 gp41. *Science* **274:** 1917–1921.

Armitage RJ, Maliszewski CR, Alderson MR, Grabstein KH, Spriggs MK, Fanslow WC (1993). CD40L: a multifunctional ligand. *Semin Immunol* **5:** 401–412.

Banchereau J, Steinman RM (1998). Dendritic cells and the control of immunity. *Nature* **392:** 245–252.

Beebe AM, Dua N, Faith TG, Moore PF, Pedersen NC, Dandekar S (1994). Primary stage of feline immunodeficiency virus infection: viral dissemination and cellular targets. *J Virol* **68:** 3080–3091.

Bragg DC, Meeker RB, Duff BA, English RV, Tompkins MB (1999). Neurotoxicity of FIV and FIV envelope protein in feline cortical cultures. *Brain Res* **816:** 431–437.

Bragg DC, Robertson K, Hall CD, Meeker RB (2000). Techniques to measure neurologic disease progression in HIV-1 patients. Science Online: *NeuroAIDS* **3:** 1–9.

Caux C, Massacrier C, Vanbervliet B, Dubois B, Van Kooten C, Durand I, Banchereau J (1994). Activation of human dendritic cells through CD40 cross-linking. *J Exp Med* **180:** 1263–1272.

Conant K, Garzino-Demo A, Nath A, McArthur JC, Halliday W, Power C, Gallo RC, Major EO (1998). Induction of monocyte chemoattractant protein-1 in HIV-1 Tat-stimulated astrocytes and elevation in AIDS dementia. *Proc Natl Acad Sci USA* **95:** 3117–3121.

Czub S, Muller JG, Czub M, Muller-Hermelink HK (1996). Nature and sequence of simian immunodeficiency virus-induced central nervous system lesions: a kinetic study. *Acta Neuropathol (Berl)* **92:** 487–498.

Dean AF, Montgomery M, Baskerville A, Cook RW, Cranage MP, Sharpe SA, Dennis MJ, Luthert PJ, Hou S-T, Lantos PL (1993). Different patterns of neuropathological disease in rhesus monkeys infected by simian immunodeficiency virus, and their relation to the humoral immune response. *Neuropathol Appl Neurobiol* **19:** 336–345.

Dow SW, Dreitz MJ, Hoover EA (1992). Feline immunodeficiency virus neurotropism: evidence that astrocytes and microglia are the primary target cells. *Vet Immunol Immunopathol* **35:** 23–35.

English R, Johnson C, Gebhard DH, Tompkins MB (1993). *In vivo* lymphocyte tropism of feline immunodeficiency virus. *J Virol* **67:** 5175–5186.

Everall IP, Luthert PJ, Lantos PL (1993). Neuronal number and volume alterations in the neocortex of HIV infected individuals. *J Neurol Neurosurg Psych* **56:** 481–486.

Falangola MF, Hanly A, Galvao-Castro B, Petito CK (1995). HIV infection of human choroid plexus: a possible mechanism of viral entry into the CNS. *J Neuropathol Exp Sci* **54:** 497–503.

Gabuzda DH, Ho DD, de la Monde SM, Hirsh MS, Rota TR, Sobel RA (1986). Immunohistochemical identification of HTLV-III antigen in brains of patients with AIDS. *Ann Neurol* **20:** 289–295.

Gelbard HA, Nottet HS, Swindells S, Jett M, Dzenko KA, Genis P, White R, Wang L, Choi Y-B, Zhang D, Lipton SA, Tourtellotte WW, Epstein LG, Gendelman HE (1994). Platelet-activating factor: a candidate human immunodeficiency virus type 1-induced neurotoxin. *J Virol* **68:** 4628–4635.

Gisslen M, Fuchs D, Svennerholm B, Hagberg L (1999). Cerebrospinal fluid viral load, intrathecal immunoactivation, and cerebrospinal fluid monocytic cell count in HIV-1 infection. *J Acquir Immune Defic Syndr* **21:** 271–276.

Giulian D, Vaca K, Noonan CA (1990). Secretion of neurotoxins by mononuclear phagocytes infected with HIV-1. *Science* **250:** 1593–1596.

Giulian D, Yu J, Li X, Tom D, Li J, Wendt E, Lin S-N, Schwarcz R, Noonan C (1996). Study of receptor-mediated neurotoxins released by HIV-1-infected mononuclear phagocytes found in human brain. *J Neurosci* **16:** 3139–3153.

Glass JD, Fedor H, Wesselingh SL, McArthur JC (1995). Immunocytochemical quantitation of human immunodeficiency virus in the brain: correlations with dementia. *Ann Neurol* **38:** 755–762.

Gray F, Hurtrel M, Hurtrel B (1996). Early central nervous system changes in human immunodeficiency virus (HIV)-infection. *Neuropathol Appl Neurobiol* **19:** 3–9.

Hanly A, Petito CK (1998). HLA-DR-positive dendritic cells of the normal human choroid plexus. A potential reservoir of HIV in the central nervous system. *Human Pathol* **29:** 88–93.

Heyes MP, Saito K, Lackner A, Wiley CA, Achim CL, Markey SP (1998). Sources of the neurotoxin quinolinic acid in the brain of HIV-1-infected patients and retrovirus-infected macaques. *FASEB J* **12:** 881–896.

Koenig S, Gendelman HE, Orenstein JM, Dal Canto MC, Pezeshkpour GH, Yungbluth M, Janotta F, Aksamit A, Martin MA, Fauci AS (1986). Detection of AIDS virus in macrophages in brain tissue from AIDS patients with encephalopathy. *Science* **233:** 1089–1093.

Kornbluth RS (2000). The emerging role of CD40 ligand in HIV infection. *J Leukoc Biol* **68:** 373–382.

Lackner AA, Smith MO, Munn RJ, Martfeld DJ, Gardner MB, Marx PA, Dandekar S (1991). Localization of simian immunodeficiency virus in the central nervous system of rhesus monkeys. *Am J Pathol* **139:** 609–621.

Lafrenie RM, Wahl LM, Epstein JS, Hewlett IK, Yamada KM, Dhawan S (1996). HIV-1-Tat protein promotes chemotaxis and invasive behavior by monocytes. *J Immunol* **157:** 974–977.

Lane JH, Tarantal AF, Pauley D, Marthas M, Miller CJ, Lackner AA (1996). Localization of simian immunodeficiency virus nucleic acid and antigen in brains of fetal macaques inoculated in utero. *Am J Pathol* **149:** 1097–1104.

Ling EA (1979). Ultrastruct and origin of epiplexus cells in the telencephalic choroid plexus of postnatal rats studied by intravenous injection of carbon particles. *J Anat* **129:** 479–492.

Ling EA, Kaur C, Lu J (1998). Origin, nature, and some functional considerations of intraventricular macrophages, with special reference to the epiplexus cells. *Microsc Res Tech* **41:** 43–56.

Lipton S (1992). Requirement of macrophages in neuronal injury induced by HIV envelope protein gp120. *NeuroReport* **3:** 913–915.

Lu J, Kaur C, Ling EA (1993). Intraventricular macrophages in the lateral ventricles with special reference to epiplexus cells: a quantitative analysis and their uptake of fluorescent tracer injected intraperitoneally in rats of different ages. *J Anat* **183**(Pt 2): 405–414.

Magnuson D, Knudsen B, Geiger J, Brownstone R, Nath A (1995). Human immunodeficiecy virus type 1 Tat activates non-*N*-methyl-D-aspartate excitatory amino acid receptors and causes neurotoxicity. *Ann Neurol* **37:** 373–380.

Martin C, Albert J, Hansson P, Pehrsson P, Link H, Sonnerborg A (1998). Cerebrospinal fluid mononuclear cell counts influence CSF HIV-1 RNA levels. *J Acquir Immune Defic Syndr Hum Retrovirol* **17:** 214–219.

Matyszak MK, Lawson LJ, Perry VH, Gordon S (1992). Stromal macrophages of the choroid plexus situated at an interface between the brain and peripheral immune system constitutively express major histocompatibility class 2 antigens. *J Neuroimmunol* **40:** 173–182.

Matyszak MK, Perry V (1996). The potential role of dendritic cells in immune-mediated inflammatory diseases of the central nervous system. *Neuroscience* **74:** 599–608.

McArthur JC, Sipos E, Cornblath DR, Welch D, Chupp M, Griffin DE, Johnson RT (1989). Identification of mononuclear cells in CSF of patients with HIV infection. *Neurology* **39:** 66–70.

McMenamin PG (1999). Distribution and phenotype of dendritic cells and resident tissue macrophages in the dura mater, leptomeninges, and choroid plexus of the rat brain as demonstrated in wholemount preparations. *J Comp Neurol* **405:** 553–562.

Meeker RB, Azuma Y, Bragg DC, English RV, Tompkins M (1999a). Microglial proliferation in cortical neural cultures exposed to feline immunodeficiency virus. *J Neuroimmunol* **101:** 15–26.

Meeker RB, English R, Tompkins M (1996). Enhanced excitotoxicity in primary feline neural cultures exposed to feline immunodeficiency virus (FIV). *J NeuroAIDS* **1:** 1–27.

Meeker RB, Robertson K, Barry T, Hall C (1999b). Neurotoxicity of CSF from HIV-infected humans. *J NeuroVirol* **5:** 507–518.

Meeker RB, Thiede BA, Hall C, English R, Tompkins M (1997). Cortical cell loss in asymptomatic cats experimentally infected with feline immunodeficiency virus. *AIDS Res Hum Retroviruses* **13:** 1131–1140.

Nath A, Geiger J (1998). Neurobiological aspects of human immunodeficiency virus infection: neurotoxic mechanisms. *Prog Neurobiol* **54:** 19–33.

Navia BA, Cho ES, Petito CK, Price RW (1986). The AIDS dementia complex: II. Neuropathology. *Ann Neurol* **19:** 525–535.

Nottet HSLM, Persidsky Y, Sasseville VG, Nukuna AN, Bock P, Zhai Q, Sharer LR, McComb RD, Swindells S, Soderland C, Gendelman HE (1996). Mechanisms for the transendothelial migration of HIV-1-infected monocytes into brain. *J Immunol* **156:** 1284–1295.

Persidsky Y, Stins M, Way D, Witte MH, Weinand M, Kim KS, Bock P, Gendelman HE, Fiala M (1997). A model for monocyte migration through the blood–brain barrier during HIV-1 encephalitis. *J Immunol* **158:** 3499–3510.

Petito CK, Chen H, Mastri AR, Torres-Munoz J, Roberts B, Wood C (1999). HIV infection of choroid plexus in AIDS and asymptomatic HIV-infected patients suggests that the choroid plexus may be a reservoir of productive infection. *J NeuroVirol* **5:** 670–677.

Podell M, Maruyama K, Smith M, Hayes KA, Buck WR, Ruehlmann DS, Mathes LE (1999). Frontal lobe neuronal injury correlates to altered function in FIV- infected cats. *J Acquir Immune Defic Syndr* **22:** 10–18.

Poli A, Pistello M, Carli MA, Abramo F, Mancuso G, Nicoletti E, Bendinelli M (1999). Tumor necrosis factor-alpha and virus expression in the central nervous system of cats infected with feline immunodeficiency virus. *J NeuroVirol* **5:** 465–473.

Pulliam L, Herndier BG, Tang NM, McGrath MS (1991). Human immunodeficiency virus-infected macrophages produce soluble factors that cause histological and neurochemical alterations in cultured human brains. *J Clin Invest* **87:** 503–512.

Rausch DM, Heyes MP, Murray EA, Lendvay J, Sharer LR, Ward JM, Rehm S, Nohr D, Weihe E, Eiden LE (1994). Cytopathologic and neurochemical correlates of progression to motor/cognitive impairment in SIV-infected rhesus monkeys. *J Neuropathol Exp Neurol* **53:** 165–175.

Rottman JB, Tompkins WA, Tompkins MB (1996). A reverse transcription-quantitative competitive polymerase chain reaction (RT-qcPCR) technique to measure cytokine gene expression in domestic mammals. *Vet Pathol* **33:** 242–248.

Serot JM, Foliguet B, Bene MC, Faure GC (1997). Ultrastructural and immunohistological evidence for dendritic-like cells within human choroid plexus epithelium. *NeuroReport* **8:** 1995–1998.

Sopper S, Demuth M, Stahl-Hennig C, Hunsmann G, Plesker R, Coulibaly C, Czub S, Ceska M, Koutsilieri E, Riederer P, Brinkmann R, Katz M, ter Meulen V (1996). The effect of simian immunodeficiency virus infection *in vitro* and *in vivo* on the cytokine production of isolated microglia and peripheral macrophages from rhesus monkey. *Virology* **220:** 320–329.

Steffen BJ, Breier G, Butcher EC, Schulz M, Engelhardt B (1996) ICAM-1, VCAM-1, and MAdCAM-1 are expressed on choroid plexus epithelium but not endothelium and mediate binding of lymphocytes *in vitro*. *Am J Pathol* **148:** 1819–1838.

Steigerwald ES, Sarter M, March P, Podell M (1999). Effects of feline immunodeficiency virus on cognition and behavioral function in cats. *J Acquir Immune Defic Syndr Hum Retrovirol* **20:** 411–419.

Takahashi K, Wesselingh SL, Griffin DE, McArthur JC, Johnson RT, Glass JD (1996). Localization of HIV-1 in human brain using polymerase chain reaction/*in situ* hybridization and immunohistochemistry. *Ann Neurol* **39:** 705–711.

Weiss JM, Nath A, Major EO, Berman JW (1999). HIV-1 Tat induces monocyte chemoattractant protein-1-mediated monocyte transmigration across a model of the human blood–brain barrier and up-regulates CCR5 expression on human monocytes. *J Immunol* **163:** 2953–2959.

Wesselingh SL, Takahashi K, Glass JD, McArthur JC, Griffin JW, Griffin, DE (1997). Cellular localization of tumor necrosis factor mRNA in neurological tissue from HIV-infected patients by combined reverse transcriptase/polymerase chain reaction *in situ* hybridization and immunohistochemistry. *J Neuroimmunol* **74:** 1–8.

Wiley C, Masliah E, Morey M, Lemere C, DeTeresa R, Grafe M, Hansen L, Terry R (1991). Neocortical damage during HIV infection. *Ann Neurol* **29:** 651–657.

Wolburg K, Gerhardt H, Schulz M, Wolburg H, Engelhardt B (1999). Ultrastructural localization of adhesion molecules in the healthy and inflamed choroid plexus of the mouse. *Cell Tissue Res* **296:** 259–269.

Xiong H, Zeng YC, Lewis T, Zheng J, Persidsky Y, Gendelman HE (2000). HIV-1 infected mononuclear phagocyte secretory products affect neuronal physiology leading to cellular demise: relevance for HIV-1-associated dementia. *J NeuroVirol* **6**(Suppl 1): S14–S23.

Yang J-S, English RV, Ritchey JW, Davidson MG, Wasmoen T, Levy JK, Gebhard DH, Tompkins MB, Tompkins WAF (1996). Molecularly cloned feline immunodeficiency virus NCSU1 JSY3 induces immunodeficiency in specific-pathogen-free cats. *J Virol* **70:** 3011–3017.

Yeung MC, Pulliam L, Lau AS (1995). The HIV envelope protein gp120 is toxic to human brain-cell cultures through the induction of interleukin-6 and tumor necrosis factor-alpha. *AIDS* **9:** 137–143.